Proc. Natl. Acad. Sci. USA
Vol. 94, pp. 2874–2879, April 1997
Biochemistry

Crystal structure of varicella-zoster virus protease

XIAYANG QIU*, CHERYL A. JANSON†, JEFFREY S. CULP†, SUSAN B. RICHARDSON‡, CHRISTINE DEBOUCK‡, WARD W. SMITH*, AND SHERIN S. ABDEL-MEGUID*§

Departments of *Macromolecular Sciences, †Protein Biochemistry, and ‡Molecular Genetics, SmithKline Beecham Pharmaceuticals, King of Prussia, PA 19406

Communicated by William N. Lipscomb, Harvard University, Cambridge, MA, January 27, 1997 (received for review October 28, 1996)

ABSTRACT **Varicella-zoster virus (VZV), an α-herpes virus, is the causative agent of chickenpox, shingles, and postherpetic neuralgia. The three-dimensional crystal structure of the serine protease from VZV has been determined at 3.0-Å resolution. The VZV protease is essential for the life cycle of the virus and is a potential target for therapeutic intervention. The structure reveals an overall fold that is similar to that recently reported for the serine protease from cytomegalovirus (CMV), a herpes virus of the β subfamily. The VZV protease structure provides further evidence to support the finding that herpes virus proteases have a fold and active site distinct from other serine proteases. The VZV protease catalytic triad consists of a serine and two histidines. The distal histidine is proposed to properly orient the proximal histidine. The identification of an α-helical segment in the VZV protease that was mostly disordered in the CMV protease provides a better definition of the postulated active site cavity and reveals an elastase-like S′ region. Structural differences between the VZV and CMV proteases also suggest potential differences in their oligomerization states.**

Members of the human herpes virus family are responsible for a variety of diseases from subclinical infections to fatal diseases in the immunocompromised or immunosuppressed. The family is divided into three subfamilies designated α, β, and γ. The α subfamily includes herpes simplex viruses 1 and 2 (HSV-1 and HSV-2) and varicella-zoster virus (VZV); the β subfamily includes cytomegalovirus (CMV) and human herpes viruses 6 and 7; and the γ subfamily includes Epstein–Barr virus and human herpes virus 8. Viruses of the α subfamily are among those causing serious diseases. HSV-1 is the virus responsible for herpes labialis (cold sores), whereas HSV-2 causes genital herpes. VZV is a neurotropic α-herpes virus responsible for chickenpox, shingles, and postherpetic neuralgia: primary exposure to the virus results in chickenpox, reactivation of the virus after a period of latency gives rise to shingles, and postherpetic neuralgia is probably the result of nerve damage during the active replication phase of shingles (1).

An essential step in herpes virus assembly (2) is the proteolytic processing of an assemblin protein designated ICP35 in HSV-1 (3). Processing of the assemblin protein is catalyzed by a virally encoded serine protease that contains the assemblin protein at its C terminus (3). This protease catalyzes its own cleavage to produce an N-terminal domain having full catalytic activity (4, 5). Herpes protease domains show significant sequence homology within each subfamily, but only very limited homology between different subfamilies (Fig. 1, Table 1). For example, the VZV protease shows 50% identity to HSV-1 and HSV-2 proteases, but only 26% to CMV protease. There is little sequence homology to other known proteins, including the absence of the conserved G-X-S/C-G-G sequence for chymotrypsin-like and G-T-S-M/A for subtilisin-like proteases. All human herpes virus proteases cleave a peptide bond between an alanine and a serine (6). Differences in substrate specificity exist. For example, HSV-1 protease cannot cleave the protein substrate of CMV protease, but the CMV protease can cleave that of HSV-1 protease (7).

Recently the crystal structure of CMV protease has been reported (8–11). The structure reveals a new fold that has not been reported for any other serine protease, and an active site consisting of a novel catalytic triad in which the third member of the triad is a histidine instead of an aspartic acid. The structure also suggests a catalytic tetrad composed of a serine, two histidines, and an aspartic acid. The limited sequence homology with CMV protease precluded detailed modeling of the VZV protease structure. Here we report the crystal structure of the serine protease from VZV, the first structure of the serine protease from an α-herpes virus. Comparison of the VZV and CMV protease structures should facilitate better understanding of the substrate specificity and catalytic mechanism of herpes virus proteases, and provide a structural basis for the rational design of antiviral agents.

MATERIALS AND METHODS

Crystallization and Data Acquisition. VZV protease contains 605 residues, of which residues 1–236 (protease domain) have full catalytic activity. The molecule used in this study contains only amino acids 10–236, in which the cysteine at position 10 of the authentic sequence (12) has been replaced by a methionine for *Escherichia coli* expression. These changes do not alter the protease activity. The VZV protease was purified from *E. coli* cells using Ni-NTA-agarose (Qiagen, Chatsworth, CA) and Superdex 75 (Pharmacia) chromatographies (J.S.C., unpublished data). A small portion of the final VZV protease product is 717 daltons less than expected as detected by matrix-associated laser desorption ionization mass spectrometry, corresponding to a six amino acid deletion from the C terminal. Crystals were grown by the method of vapor diffusion in hanging drops using 0.1 M phosphate buffer (pH 6.2) containing 2.5 M NaCl as precipitant and 10 mg/ml protein mixed 1:1 with the precipitant in the drop. The symmetry of the diffraction was consistent with that of the hexagonal space group $P6_422$ (or $P6_222$) having $a = b = 90.0$ Å and $c = 117.4$ Å. There is one molecule per asymmetric unit, with a V_M of 3.1 Å^3/Da and about 60% solvent. Diffraction data were collected with a Siemens multiwire area detector mounted on a Siemens rotating-anode x-ray generator producing graphite-monochromated CuK_α radiation and processed with the program XENGEN (13). The native data are 90% complete to 3.0 Å with an R_{merge} ($\Sigma\ I - \langle I\rangle/\Sigma\langle I\rangle$) of 0.07.

The publication costs of this article were defrayed in part by page charge payment. This article must therefore be hereby marked "*advertisement*" in accordance with 18 U.S.C. §1734 solely to indicate this fact.

0027-8424/97/942874-6$2.00/0
PNAS is available online at **http://www.pnas.org**.

Abbreviations: HSV-1, herpes simplex virus type 1; HSV-2, herpes simplex virus type 2; VZV, varicella-zoster virus; CMV, human cytomegalovirus; I site, inactivation site.

Data deposition: The atomic coordinates reported in this paper have been deposited in the Protein Data Bank, Chemistry Department, Brookhaven National Laboratory, Upton, NY 11973, accession no. 1VZV.

§To whom reprint requests should be addressed.

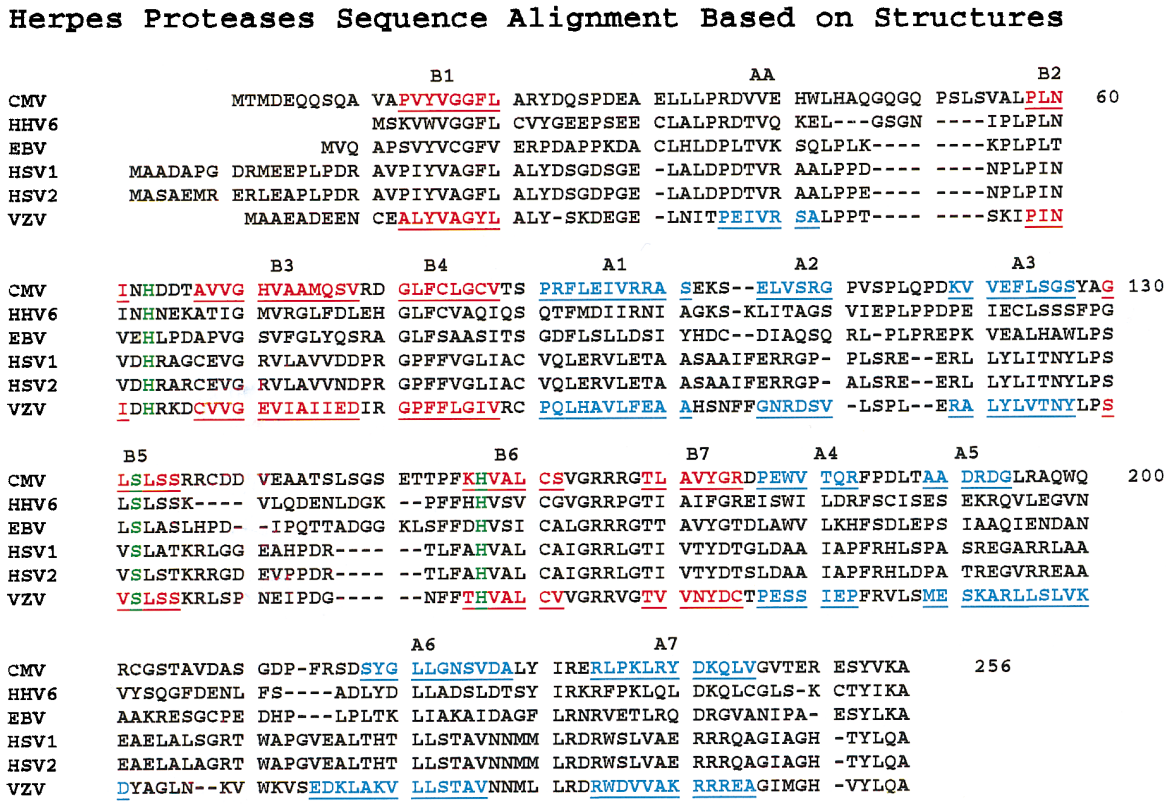

FIG. 1. The structure-assisted alignment of human herpes virus proteases. The secondary structure elements of CMV and VZV protease are underlined and labeled. Helical (AA-A7) regions (blue), strands (B1-B7) (red), and the conserved catalytic triad (green). CMV numbering is used.

Heavy Atom Derivatives. To identify heavy atom derivatives 36 different compounds were screened, each at several different concentrations. The presence of the slightest amount of mercury destroyed the crystals. Two poor derivatives finally were obtained by soaking a crystal in 1 mM potassium gold cyanide for 1 day, and another in 2 mM trimethyllead acetate for 3 days. The gold data set was 81% complete to 4.5 Å with an R_{merge} of 0.14 and R_{iso} ($\Sigma\ |FPH - FP|/\Sigma|FH_o|$) of 0.19, while the lead was 92% complete to 4.2 Å with an R_{merge} of 0.20 and R_{iso} of 0.17. The gold binding site was identified by difference Patterson methods using programs from CCP4 (14). The lead site, at a position similar to the gold, could be seen only by difference Fourier methods. The phasing power and R_{Cullis} ($\Sigma |FH_o - FH_c|/\Sigma|FH_o|$) of the gold derivative were 1.2 and 0.79 and those of the lead derivative were 1.0 and 0.82, respectively. The combined figure of merit was 0.37, and the resulting electron density map was not interpretable.

Molecular Replacement. After determining the CMV protease structure (8), molecular replacement methods were used in combination with heavy atom derivatives to solve the structure of VZV protease. Using the program XPLOR (15), a correct solution was identified only after all nonconserved regions were excluded, and nonhomologous residues were replaced by alanines in the search model. The rotation solution, obtained using 8.0–4.0 Å data, was the highest peak ($\theta1$ = 103.8°, $\theta2$ = 12.5°, $\theta3$ = 271.8°). It was 25σ above the mean and 1σ higher than the second highest peak. Translation searches were carried out in the two possible space groups $P6_122$ and $P6_422$, the latter giving a better solution (T = 27.0 Å, 13.9 Å, 19.6 Å) with a 5σ in peak height and 52.6% in R-factor for data in the 8.0–3.0 Å range. After rigid body refinement the R-factor was reduced to 50.6%. Examination of crystal packing revealed a tight dimer interface similar to that observed in the CMV protease structure (8). Using the calculated phases from the molecular replacement solution, the gold heavy atom position was found to be identical to that found from the difference Patterson, further confirming the correctness of the molecular replacement solution. However, the resulting map was still uninterpretable.

Table 1. Sequence identities (%) between herpes virus proteases

	CMV	VZV	HSV2	HSV1	HHV6	EBV
CMV	—	**26**	**26**	**26**	**38**	**31**
VZV	*30*	—	**52**	**50**	**21**	**23**
HSV2	*30*	*54*	—	**91**	**23**	**27**
HSV1	*30*	*54*	*91*	—	**23**	**26**
HHV6	*41*	*21*	*24*	*24*	—	**31**
EBV	*34*	*26*	*31*	*31*	*29*	—

Bold, from Fig. 1; italic, from GCG, slightly different because structure information was not used in sequence alignments.

Structure Solution and Refinement. The crystal structure of VZV protease was solved by combining phases from the two heavy atom derivatives and the molecular replacement solution. The combined overall figure of merit was 0.39 for data to 3.0 Å resolution. Although the electron density map was still noisy, the phases were good enough to give a very clear electron density map after solvent flattening and histogram matching (14) using 60% solvent, with R_{free} decreased from 53.7% to 36.8%. Cycles of model building with XTALVIEW (16) and refinement with XPLOR produced a final model of 211 amino acids. Fifteen residues were disordered in the crystal structure: residues 138–153 and 252–256 (CMV protease numbering¶). A total of 4,903 reflections were included in the final refinement (7.0–3.0 Å), giving an R-factor ($\Sigma |F_o - F_c|/\Sigma F_o$) of 22.3% without refining temperature factors or

¶In this work, we will use CMV protease numbering (as shown in Fig. 1) to describe all VZV protease residues. In most cases the VZV protease numbers will be shown in "{}" brackets. This should eliminate any future confusion and will help standardize numbering of catalytic triad residues as has been done with the trypsin family of serine proteases.

adding solvent molecules. The rms deviations are: bond length 0.014 Å, bond angle 2.1°, dihedral angle 25.1°, and improper angle 1.8°. His63{52} and His157{139} were refined as carrying a single proton at the ND1 atom. The estimated coordinates error is 0.4 Å using the SIGMAA method (17). The program PROCHECK (18) was used to check for stereochemical and geometrical outliers in the final structure, and the results indicate good quality. The Ramachandran plot shows 80% in most favored, 17% in additionally allowed, 1.5% in generously allowed, and 1.5% in disallowed regions.

RESULTS AND DISCUSSION

Overall Structure. Unlike the structures of classical serine proteases having two distinct β-barrel domains, VZV protease is a single domain protein. It can be described as a seven-stranded orthogonally packed β-barrel core surrounded by eight helices and connecting loops (Fig. 2*A*). The core β-barrel is mostly antiparallel, except strands B2 and B6, which are parallel. Despite limited sequence identity (26%; Table 1), the overall fold of VZV protease is found to be similar to that of CMV protease (8–11). The core β-barrel of the VZV protease superimposes very well with that of the CMV protease (Fig. 2*B*). The rms difference between the 52 pairs of α-carbon atoms comprising the two β-barrels is 0.7 Å, with the maximum displacement being 2.2 Å. Based on this structural superposition (Fig. 2*B*), we were able to propose a structure-assisted sequence alignment (Fig. 1). Superposition of the 142 equivalent α-carbon atoms from the two structures gives a rms deviation of 1.3 Å. More significant conformational differences between the two structures are seen in helical and loop regions. The most notable is the large movement of helices A1-A2 (Fig. 2*B*). There are also differences in the length of helix A6 at both the N and C terminus (Fig. 1). These differences may have significant impact on the oligomerization state of these molecules, as will be discussed later. An additional loop containing a small α-helix (Fig. 1; referred to as AA loop) has been observed in the VZV protease structure (Fig. 2*A* in red). The corresponding segment in the CMV protease is nine residues longer (Fig. 1) and was either totally or partially disordered in CMV protease structures (8–11).

Dimer Interface. It has been shown (20, 21) that the active species of CMV protease is a dimer. A dimer also has been identified in the crystal structure of the CMV protease (8–11).

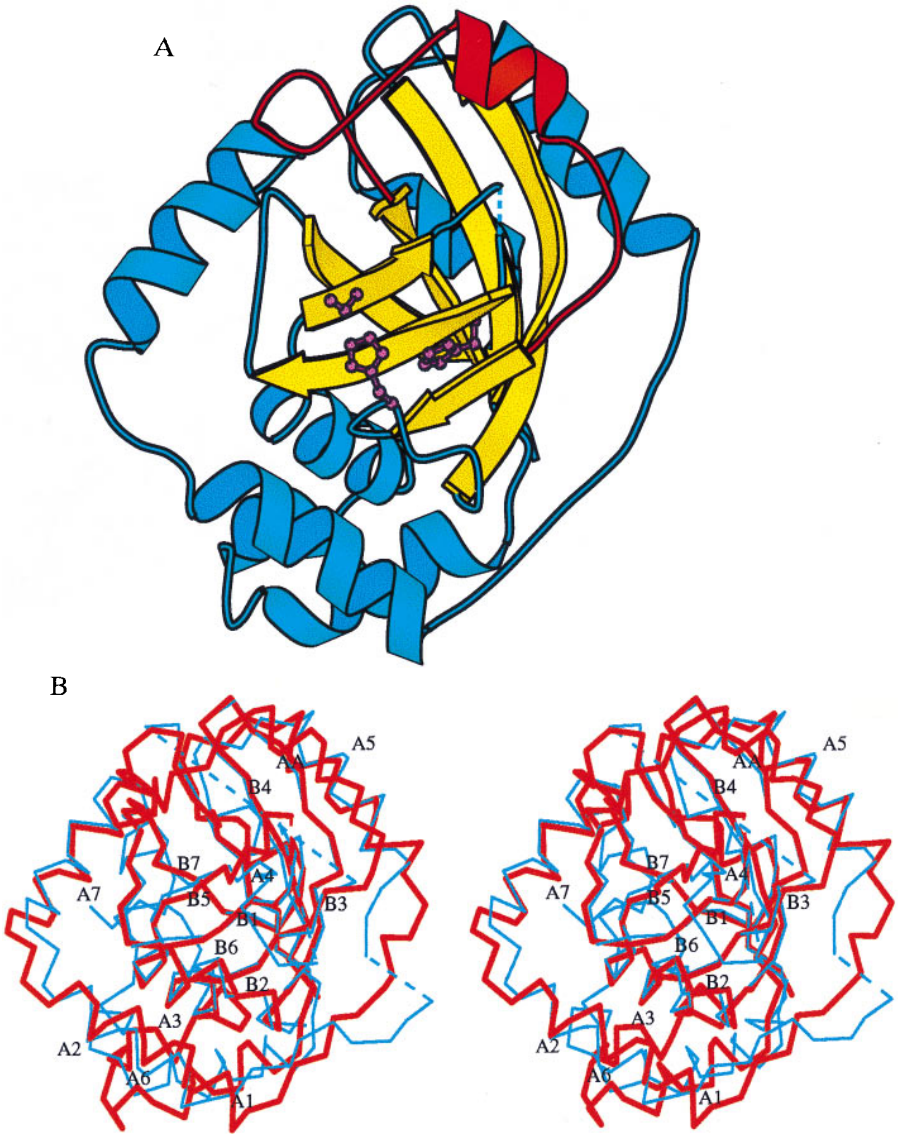

FIG. 2. The monomeric structure of the VZV protease. (*A*) The core β-barrel (yellow), the catalytic triad (purple), and the AA loop (red). (*B*) Stereoview of the superposition between the VZV (thick red lines) and CMV (thin blue lines) protease structures. The secondary elements of the VZV protease are labeled. The diagram was drawn with the program MOLSCRIPT (19).

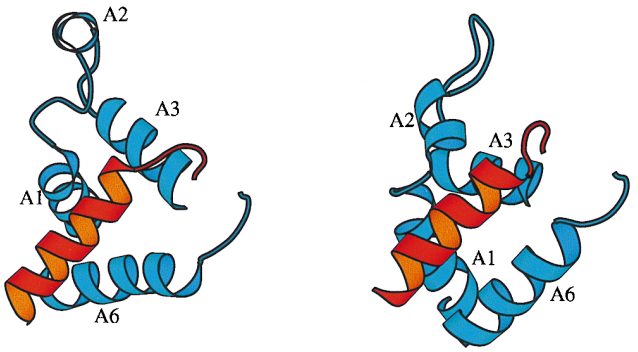

FIG. 3. (*Left*) The dimer interface of VZV protease. (*Right*) CMV protease. Helix A6 of one of the monomers is shown in red; A1, A2, A3, and A6 of the other are shown in blue. The two A6 helices are not parallel to each other in VZV protease. The segments containing helices A2 assume quite different conformations in VZV and CMV proteases.

There is no report on the dimer formation of any α-herpes virus protease, but the conservation of amino acid sequences (Fig. 1) and enhancement of catalytic activity seen in the presence of aggregation-promoting agents such as glycerol and citrate (22) suggest similar dimerization of all herpes proteases. Indeed, dimers in which the monomers are related by 2-fold crystallographic axes have been identified for VZV protease (Fig. 3). Similar to CMV protease, the VZV protease dimer interface contains four helices (A1, A2, A3, and A6) of one monomer surrounding helix A6 of the other monomer. The interface area between the two monomers is about 1,300 Å^2, comparable to that of the CMV protease.

There are many notable structural differences in the dimer interfaces of VZV and CMV proteases. Helices A6 from each monomer were reported to be almost parallel in the CMV protease structure (8), but show about a 30° twist in the VZV protease structure (Fig. 3). Helix A6 in VZV protease is one turn longer at its N terminus, and a half-turn shorter at its C terminus. The loop connecting A5 and A6 is also quite different in the two structures (Fig. 2*B*). The biggest difference between these two structures resides in the segment containing helix A2 (Fig. 3). In the structure of CMV protease, this segment assumed a "closed" conformation, making intramolecular contacts and forming part of the dimer interface (8). In the VZV protease crystals, this segment adopts an "open" conformation (Figs. 2*B* and 3), interacting only with another symmetry-related molecule to form a different dimer interface. Therefore, compared with the CMV protease, VZV protease may have a different oligomerization state. The opened conformation of the helix A2 segment may be used to form protein-protein interaction among α-herpes virus protease molecules and to construct higher order oligomers, e.g., tetramers. While there is mostly monomer-dimer equilibrium in CMV protease solution, we believe that the α-herpes virus proteases could have a monomer-dimer-tetramer equilibrium in solution.

The core β-barrels are well conserved among α- and β-herpes virus proteases, but large differences exist in their dimer interfaces. Because the interface is distal to the catalytic triad (Fig. 2), dimerization must indirectly influence catalytic activity. Helix A6, the core of the dimer interface, is directly involved in forming parts of the S′ subsites. In the absence of dimer formation, it is possible that helix A6 moves toward the active site to block ligand access and/or change the shape of

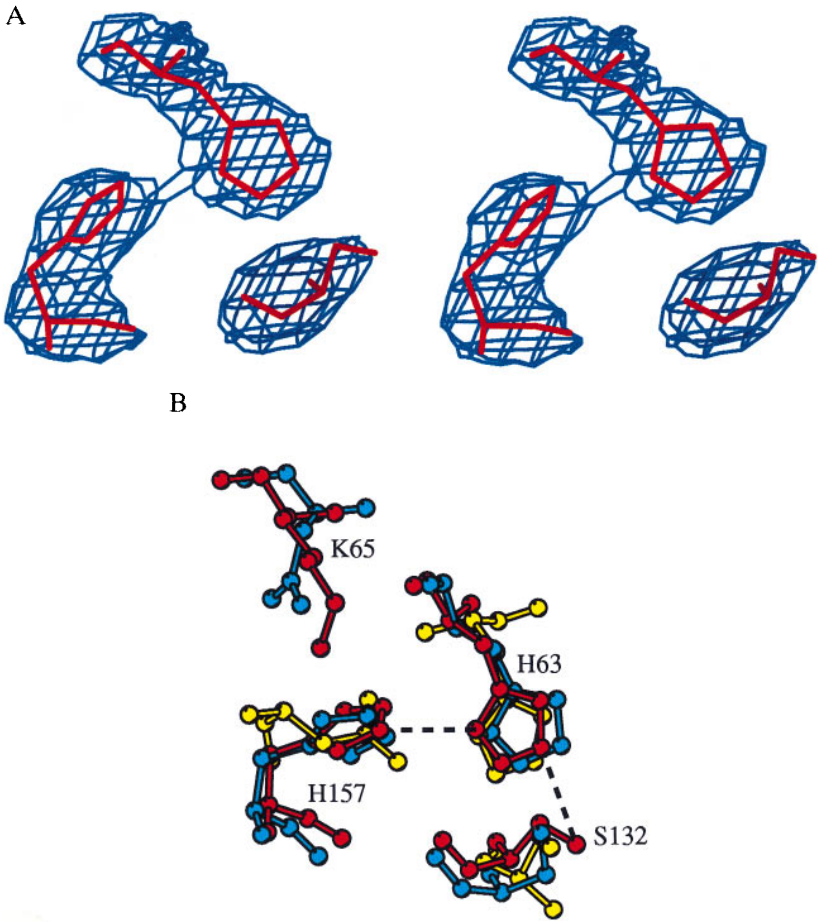

FIG. 4. The catalytic residues (*A*) in the omit $F_o - F_c$ map contoured at 3σ. (*B*) VZV protease (red) compared with CMV (blue) and trypsin (yellow). Dashed lines connects the catalytic triad of the VZV protease. Only CMV numbering is used.

the active site cavity, thus rendering the enzyme inactive or much less active.

Catalytic Triad and Mechanism. The active site of the VZV protease is situated in the only region of the core β-barrel that is not sheltered by helices and flanking loops (Fig. 2*A*). The active site region is very shallow with the catalytic residues rather exposed to solvent. This shallowness is not unreasonable considering the P1-P1′ residues (Ala-Ser) are small. Biochemical and mutational analysis on various α- and β-herpes viruses (5, 23, 24) had identified Ser132{120} and His63{52} as members of the catalytic triad. From the crystal structure of the CMV protease, compelling geometrical evidence suggested His157, instead of an aspartic or glutamic acid, as the third catalytic triad residue (8). One concern was a report in which His157 was mutated to an alanine, indicating that His157 is important, but not essential to the activity of CMV protease (24). In the VZV protease structure, a similar Ser-His-His catalytic triad also was identified, with His157{139} being the third catalytic residue (Fig. 4). Considering that His157 is absolutely conserved among all herpes proteases, we believe that it plays a critical role in catalysis of the herpes proteases. The residual activity remaining in the His157Ala mutant of CMV protease could be attributed to remaining binding determinants that stabilize the transition state complex as has been proposed (25) for the classical serine proteases. In fact, a Ser-His catalytic diad of a catalytic antibody was found to be sufficient for catalyzing the hydrolysis of L-amino acid esters (26).

Given that the third member of the catalytic triad is a histidine instead of an aspartic acid, its role in the catalytic mechanism should be addressed. In the VZV protease structure, the triad geometry suggests that each of His63{52} and His157{139} carries a single proton on ND1, which is quite reasonable at this enzyme's optimal pH 8.0 (27). There are two common models for the mechanism of classical serine proteases (see ref. 25 for a recent review). One is the "two-proton transfer model," in which the Asp accepts the second proton to become uncharged in the transition state. In such a model, it would be quite difficult for a histidine to play the role of the aspartic acid. In the second model, supported by recent data (25), the most important role for the Asp seems to be the ground-state stabilization of the required tautomer and rotamer of the catalytic proximal histidine. This appears to be a role that is played by His157{139} in the VZV protease structure. A His-His interaction may have less rotameric orientations than that of His-Asp, which might be relevant to the stability of the triad in such an exposed catalytic cavity. In either mechanistic model, His63{52} would acquire a proton in the transition state and thus become positively charged. Unlike an aspartic acid, His157{139} will not be able to compensate for this developing positive charge, but could further delocalize it. However, it is reasonable to assume that having a second histidine instead of an aspartic acid in the triad would result in a decreased catalytic efficiency. This is supported by the fact that all herpes virus proteases are rather slow enzymes (20–22).

The structure of CMV protease also contains an aspartic acid proximal to the second histidine and an alternative possibility is that the catalytic apparatus is a tetrad composed of Ser132, His63, His157, and Asp65 (8). Asp65 is rather flexible in the CMV protease structure; it is replaced by a lysine in VZV protease and alanines in HSV-1 and HSV-2 proteases (Fig. 1). It is possible, however, that the role that Asp65 may play in CMV protease could be substituted by another residue in VZV protease. Inspection of the VZV protease crystal structure in the vicinity of residue 65{54} indicates no such substitution. Lys65{54} in VZV protease is found with its side-chain nitrogen more than 5 Å away from His63{52} and would not be a suitable substitution for an aspartic acid. Although it may be possible that residue 65 contributes to CMV protease catalytic activity, but not to that of VZV, the structure of the latter enzyme confirms the essential and conserved feature of the active site as being a novel Ser-His-His catalytic triad. Whether a Ser-His-His-Asp catalytic tetrad is more active awaits further kinetic studies.

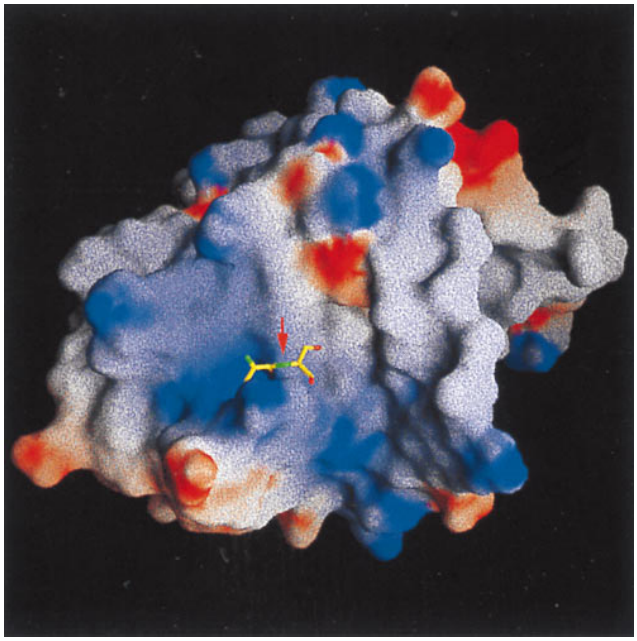

FIG. 5. Molecular surface of the VZV protease looking into the postulated substrate binding groove. The surface is color-coded by electrostatic potentials (blue for positive and red for negative) calculated with the program GRASP (28). Modeled is the Ala-Ser cleavage site. The red arrow indicates the position of the scissile bond.

Substrate Binding. There are 15 residues that are disordered in the VZV protease structure. Ten of them (138–153){127–136} are in the surface loop that corresponds to the CMV protease "I (inactivation) site" (6, 24) and probably will become ordered in the presence of a substrate. The other five residues are at the C terminal (252–256){232–236}, probably a consequence of the absence of the last six residues from a small portion of the protein used to obtain our crystals (see *Materials and Methods*).

The I site loop and a large segment containing residues 25–55 were mostly disordered in our CMV protease structure (8). The region corresponding to the latter segment (red in Fig. 2*A*; AA loop) is ordered in the VZV protease structure. The amino acid sequences in these two regions are not very conserved among proteases from various herpes viruses, with the CMV protease having multiresidue insertions in both regions (Fig. 1). An I site deletion mutant of CMV protease was shown to have altered substrate specificity (23). Given the proximity of these loops to the active site, it was suggested that they are important for substrate recognition (8).

Subsite specificity beyond P1-P1′ sites are important in substrate recognition of herpes virus proteases. It has been shown that CMV protease can cleave the protein substrate of the HSV-1 enzyme, but the latter cannot cleave that of the CMV enzyme (7). Among the various herpes virus proteases, the unprimed substrate sites showed greater consensus sequence than the primed ones (6). Although differences exist between the VZV and CMV protease structures, the active site geometry is well conserved between them (Fig. 4). Despite a totally different protein fold of the herpes virus proteases when compared with the classical serine proteases, the catalytic triad residues as well as the proposed oxyanion hole are quite superimposable (8). Given the absence of the two aforementioned loop segments around the CMV protease active site, it was difficult to define that protease active site cavity. With the

VZV protease structure, one of the large loops (that containing residues 25–55) is ordered, and the structure has a much better defined active site cavity (Fig. 5).

There is a shallow groove running across the catalytic site. The right side of the groove is relatively wide and deep (Fig. 5). It is defined by the end of helix A6, the end of strand B6, His63{52} and the highly conserved Gly-Arg-Arg{146–148} segment. Superimposing the Ser-His catalytic dyad of human leukocyte elastase (29) and the VZV protease shows that this side of the VZV protease groove is similar to the S′ cavity of elastase, with the P1′-P3′ residues of the turkey ovomucoid inhibitor able to fit well in the VZV protease groove. The left side of the active site groove is rather narrow. This region could be the unprimed subsites (S subsites) of the VZV protease and is delineated by strand B5, the Gly-Arg-Arg segment, and the beginning of the AA loop. Because strand B5 is almost parallel to this groove, it is possible that the substrate peptide could be inserted into the groove with its main chain in an extended conformation forming an antiparallel β-sheet with strands B5 and B6. Fig. 5 shows an approximate position of the P1-P1′ peptide in the VZV protease active site cavity. In this model the AA loop is important for forming the S2-S4 subsites, and the I site loop could be important for recognizing substrate residues P4 and further. Therefore, the difference in substrate specificity between α- and β-herpes virus proteases could be explained by the large differences in these loop regions. Structures of protease-ligand complexes are needed to support this model.

The structure of VZV protease provides the first direct structural information about an α-herpes virus protease. It documents the conservation of the overall fold among herpes proteases and shows differences in the monomeric and dimeric forms of these enzymes. It provides new evidence to confirm the novel Ser-His-His catalytic triad and a better understanding of the catalytic mechanism and substrate specificity of this new class of proteases, which forms an important basis for structure-based drug design.

We thank Lyn Gorniak and Arun Patel for activity assays, Jim Kane for fermentation studies, George Glover, Richard Jarvest, Hiro Nishikawa, and Martin Rosenberg for encouragement and support, and Cathy Peishoff for useful discussions.

1. Straus, S. E. (1994) *Ann. Neurol.* **35,** S11–S12.
2. Gao, M., Matusick-Kumar, L., Hurlburt, W., DiTusa, S. F., Newcomb, W. W., Brown, J. C., McCann, P. J., III, Deckman, I. & Colonno, R. J. (1994) *J. Virol.* **68,** 3702–3712.
3. Liu, F. & Roizman, B. (1991) *J. Virol.* **65,** 5149–5156.
4. Liu, F. & Roizman, B. (1993) *J. Virol.* **67,** 1300–1309.
5. Liu, F. & Roizman, B. (1992) *Proc. Natl. Acad. Sci. USA* **89,** 2076–2080.
6. McCann, P. J., III, O'Boyle, D. R., II & Deckman, I. C. (1994) *J. Virol.* **68,** 526–529.
7. Welch, A. R., Villarreal, E. C. & Gibson, W. (1995) *J. Virol.* **69,** 341–347.
8. Qiu, X., Culp, J. S., DiLella, A. G., Hellmig, B., Hoog, S. S., Janson, C. A., Smith, W. W. & Abdel-Meguid, S. S. (1996) *Nature (London)* **383,** 275–279.
9. Shieh, H.-S., Kurumbail, R. G., Stevens, A. M., Stegeman, R. A., Sturman, E. J., Pak, J. Y., Wittwer, A. J., Palmier, M. O., Wiegand, R. C., Holwerda, B. C. & Stallings, W. C. (1996) *Nature (London)* **383,** 279–282.
10. Tong, L., Qian, C., Massariol, M.-J., Bonneau, P. R., Cordingley, M. G. & Lagace, L. (1996) *Nature (London)* **383,** 272–275.
11. Ping, C., Almassy, R., Tsuge, H., Matthews, D., Pinko, C., Gribskov, C. & Kan, C.-C. (1996) *Cell* **86,** 835–843.
12. Davison, A. J. & Scott, J. E. (1986) *J. Gen. Virol.* **67,** 1759–1816.
13. Howard, A. J., Gilliland, G. L., Finzel, B. C., Poulos, T. L., Ohlendorf, D. H. & Salemme, F. R. (1987) *J. Appl. Crystallogr.* **20,** 383–387.
14. Collaborative Computational Project, No. 4 (1994) *Acta Crystallogr. D* **50,** 760–763.
15. Brunger, A. T., Kuriyan, J. & Karplus, M. (1987) *Science* **235,** 458–460.
16. McRee, D. E. (1993) *Practical Protein Crystallography* (Academic, San Diego).
17. Read, R. J. (1986) *Acta Crystallogr. A* **42,** 140–149.
18. Laskowski, R. A., MacArthur, M. W., Moss, D. S. & Thornton, J. M. (1993) *J. Appl. Crystallogr.* **26,** 283–291.
19. Kraulis P. (1991) *J. Appl. Crystallogr.* **24,** 946–950.
20. Darke, P. L., Cole, J. L., Waxman, L., Hall, D. L., Sardana, M. K. & Kuo, L. C. (1996) *J. Biol. Chem.* **271,** 7445–7449.
21. Margosiak, S. A., Vanderpool, D. L., Sisson, W., Pinko, C. & Kan, C.-C. (1996) *Biochemistry* **35,** 5300–5307.
22. Hall, D. L. & Darke, P. L. (1995) *J. Biol. Chem.* **270,** 22697–22700.
23. DiIanni, C. L., Stevens, J. T., Bolgar, M., O'Boyle, D. R., II, Weinheimer, S. P. & Colonno, R. J. (1994) *J. Biol. Chem.* **269,** 12672–12676.
24. Welch, A. R., McNally, L. M., Hall, M. R. T. & Gibson, W. (1993) *J. Virol.* **67,** 7360–7372.
25. Perona, J. J. & Craik, C. S. (1995) *Protein Sci.* **4,** 337–360.
26. Zhou, G. W., Guo, J., Huang, W., Fletterick, R. J. & Scanlan, T. S. (1994) *Science* **265,** 1059–1064.
27. DiIanni, C. L., Mapelli, C., Drier, D. A., Tsao, J., Natarajan, S., Riexinger, D., Festin, S. M., Bolgar, M., Yamanaka, G., Weinheimer, S. P., Meyers, C. A., Colonno, R. J. & Cordingley, M. G. (1993) *J. Biol. Chem.* **268,** 25449–25454.
28. Nicholls, A. & Honig, B. H. (1991) *J. Comp. Chem.* **12,** 435–445.
29. Bode, W., Wei, A. Z., Huber, R., Meyer, E., Travis, J. & Neumann, S. (1986) *EMBO J.* **5,** 2453–2458.